Published in final edited form as:
J Mol Cell Cardiol. 2010 June ; 48(6): 1071–1079. doi:10.1016/j.yjmcc.2009.10.008.

Analysis of Angiogenesis Induced by Local IGF-1 Expression after Myocardial Infarction Using MicroSPECT-CT Imaging

Lawrence W. Dobrucki[a], **Yoshiaki Tsutsumi**[b], **Leszek Kalinowski**[a,c], **Jarrod Dean**[b], **Mary Gavin**[b], **Sabyasachi Sen**[b], **Marivi Mendizabal**[d], **Albert J. Sinusas**[a], and **Ryuichi Aikawa**[b,e]

[a]Internal Medicine, Yale University School of Medicine, New Haven, CT, USA [b]Cardiovascular Research, Caritas St. Elizabeth's Medical Center, Tufts University School of Medicine, Boston, MA, USA [c]Department of Clinical Chemistry and Biochemistry, Medical University of Gdansk, Gdansk, Poland [d]GE Healthcare, Buckinghamshire, UK [e]Gene and Stem Cell Therapy, Centenary Institute, University of Sydney, Australia

Abstract

Insulin-like growth factor-1 (IGF-1) has been found to exert favorable effects on angiogenesis in prior animal studies. This study explored the long-term effect of IGF-1 on angiogenesis using microSPECT-CT in infarcted rat hearts after delivering human IGF-1 gene by adeno-associated virus (AAV). Myocardial infarction (MI) was induced in Sprague-Dawley rats by ligation of the proximal anterior coronary artery and a total of 1011 AAV-CMV-LacZ (control) or IGF-1 vectors were injected around the peri-infarct area. IGF-1 expression by AAV stably transduced heart muscle for up to 16 weeks post-MI and immunohistochemistry revealed a remarkable increase in capillary density. A ^{99m}Tc-labeled RGD peptide (NC100692, GE Healthcare) was used to assess temporal and regional αv integrin activation. Rats were injected with NC100692 followed by ^{201}Tl chloride and in vivo microSPECT-CT imaging was performed. After imaging, hearts were excised and cut for quantitative gamma-well counting (GWC). NC100692 retention was significantly increased in hypoperfused regions of both LacZ and IGF-1 rats at 4 and 16 weeks post-MI. Significantly higher activation of αv integrin was observed in IGF-1 rats at 4 weeks post treatment compared with control group, although the activation was lower in the IGF-1 group at 16 weeks.

Local IGF-1 gene delivery by AAV can render a sustained transduction and improve cardiac function post-MI. IGF-1 expression contributes to enhanced αv integrin activation which is linked to angiogenesis. MicroSPECT-CT imaging with ^{99m}Tc-NC100692 and quantitative GWC successfully assessed differences in αv integrin activation between IGF-1 treated and control animals post-MI.

Correspondence should be addressed to Albert J. Sinusas or Ryuichi Aikawa: **Albert J. Sinusas MD**, Yale University School of Medicine, Section of Cardiovascular Medicine, P.O. Box 208017, 3FMP, New Haven, CT 06520-8017, U.S.A, Tel: +1 203-785-4915, Fax: +1 203-737-1026, albert.sinusas@yale.edu, **Ryuichi Aikawa MD, PhD**, Centenary Institute, University of Sydney, Locked Bag 6, Newtown NSW 2042, Australia, Tel: +61 29565-6127, Fax: +61 29565-6101, raikawa@usyd.edu.au.

Disclosures

Marivi Mendizabal is an employee of GE Healthcare.

Keywords

AAV; IGF-1; angiogenesis; microSPECT-CT; molecular imaging; myocardial infarction

1. Introduction

Insulin-like growth factor-1 (IGF-1) is a 7.6 kDa polypeptide growth factor, which is expressed by many cells and tissues during embryonic and postnatal development and in adult animals [1–3]. IGF-1 influences various biological processes through binding to a membrane–anchored receptor (IGF-1R), although at higher concentrations, IGF-1 can also activate the insulin receptor [2]. In addition, in vivo, IGF-1 action is modulated by a family of IGF-binding proteins present in the circulation [3]. IGF-1, secreted from the liver in response to growth hormone (GH), promotes postnatal growth in bone, muscle, fat, and other tissues [1–3]. Human and murine IGF-1 deficiency causes severe intrauterine and postnatal growth retardation, perinatal lethality, delayed development in a variety of organs [1], indicating that IGF-1 is a key regulator of cell development. It has recently been reported that overexpression of IGF-1 attenuates myocyte necrosis and apoptosis after infarction in transgenic mouse model [4] and rescues cardiac myocytes from apoptosis in dilated cardiomyopathy [5]. It has also been reported that overexpression of IGF-1 improves cardiomyocyte senescence in transgenic mouse model [6] and reduces cardiomyocyte atrophy induced by ischemia [7]. Accordingly, IGF-1 has been regarded as a pleiotropic growth factor affecting myocyte proliferation and regeneration in heart development and injury.

Recent reports have further indicated that IGF-1 has a strong effect on angiogenesis [8–10], which represents the formation of neovasculature from the endothelium of preexisting vessels. It has been reported that IGF-1 can induce angiogenesis in skeletal muscle and brain tissue [9,10]. Su et al. demonstrated that IGF-1 potently induced endothelial cell migration in a matrigel assay and capillary formation in organ ring culture assay [8], which are known as important components of the angiogenic response. As systemic IGF-1 peptide administration induces unfavorable side effects such as edema and tachycardia [11], Rabinovsky et al. performed local injection of expression plasmids containing the IGF-1 gene into the skeletal muscle following femoral artery ligation in mice and demonstrated that IGF-1 treatment evoked angiogenesis and increased blood flow in the skeletal muscle. Therefore, it is plausible that local IGF-1 expression would protect cardiomyocytes from ischemia through induction of angiogenesis under conditions of ischemic injury.

Recombinant adeno-associated virus (AAV) is currently recognized as an effective gene transfer vector for heart diseases [12–14]. The physical stability of AAV makes these vectors advantageous for in vivo use, and transgene expression can persist long-term in a wide range of tissues including heart and skeletal muscle [15–17]. Recently, we reported that AAV markedly transduced cardiomyocytes in an infarcted rat heart and the transgene expression was observed up to 22 weeks [18].

Traditionally, the angiogenic response has been examined by evaluation of the physiological changes associated with the process. More recently, a number of investigators have demonstrated the feasibility of non-invasive evaluation of angiogenesis using image-based approaches targeted at cell surface receptors. We previously demonstrated the potential of single photon emission computed tomographic (SPECT) imaging with radiolabeled tracers targeted at αv integrins and X-ray computed tomography (CT) for evaluation of spatial and temporal changes in peripheral [19] and in myocardial angiogenesis in mice [20], rats, and dogs post MI [21,22].

To date there have been no reports showing the effect or mechanism of long term IGF-1 expression on angiogenesis post-MI. In this study, we examined the IGF-1 effect on angiogenesis with both biochemical assay and microSPECT-CT imaging using ^{99m}Tc-labeled peptide (NC100692, GE Healthcare) targeted at αv integrins [23], known to be activated during angiogenic process. Here we show that AAV mediated long-term stable expression of human IGF-1 in rat heart post-MI, and overexpression of IGF-1 significantly improved cardiac function and enhanced angiogenesis in the early stage after infarction.

2. Materials and methods

2.1 AAV vector production

To produce an AAV-CMV-IGF-1 construct, human IGF-1 cDNA, as defined in NCBI-X00173, was amplified by a standard polymerase chain reaction (PCR) method using IGF-1 specific PCR primers as shown below, using a human gene clone (clone ID: 984882, Catalog# 97002RG, Invitrogen™ life technologies).

5'primer: 5'-CCGAATTCTTCAGAAGCAATGGGA-3'

3'primer: 5'-CGGGATCCGTCTTCCTACATCCTG-3'

(Underlines show original IGF-1 cDNA sequence)

After the fragment of sequence was confirmed, the cDNA of IGF-1 was inserted into a type 2 pAAV-CMV vector plasmid [17]. AAV vectors were produced as described [18]. Finally, the particle titer was determined by dot blot analysis and the AAV vectors with a particle titer of 1×10^{12}/ml were prepared.

2.2 Animal studies

All procedures were performed with approval of the Institutional Animal Care and Use Committees at Caritas St. Elizabeth and Yale University. Six to eight weeks male Sprague-Dawley rats (Jackson Laboratory, Bar Harbor, Maine) were used. They were anesthetized with an intraperitoneal injection of ketamine (40–90mg/kg) and xylazine (5–10mg/kg) and the respiration was controlled using an animal ventilator for a thoracotomy incision. Myocardial infarction was induced by ligating the proximal left anterior descending coronary artery with 6-0 prolene suture. Following induction of MI, under direct visualization AAV-lacZ control or AAV-IGF-1 vector (20μl containing 2×10^{10} particles) was directly injected using a 30-gauge needle to 5 sites (total 1×10^{11} particles) of the myocardium around the infarcted area [18].

2.3 IGF-1 ELISA assay

Periodically blood samples were taken from the tail vein of anesthetized rats, for the measurement of plasma human IGF-1 levels using a human IGF-1 ELISA assay kit (Quantikine).

2.4 RT-PCR for mRNA expression and viral genome detection by regular PCR

Total RNA samples were prepared from cultured H9C2 cells and rat heart tissues with RNA-Stat (Tel-Test, #CS-111). Samples were subjected for real- time (RT)-PCR for quantification of mRNA expression using specific probe (Table 1) as described before [18]. Total DNA was extracted from tissues using Puregene DNA Isolation Kit, and then a 286-bp fragment of the AAV genome was amplified using sense primer of ITR region and antisense primer of CMV promoter [24].

Angiogenesis is stimulated by a large number of soluble angiogenic factors that regulate endothelial migration, proliferation, and survival [25]. Two of the most well studied factors,

vascular endothelial growth factor (VEGF) and basic fibroblast growth factor (bFGF), have emerged as critical regulators of the angiogenic process [26,27]. In addition, eNOS is shown as a downstream target for VEGF-induced angiogenesis, which involves activation by Akt [28] [29]. The mRNA expression of all of these critical angiogenic factors was assessed in myocardial tissue from rats in both treatment groups euthanized at 4 and 16 weeks post-MI, using established quantitative RT-PCR techniques.

2.5 Echocardiography

Transthoracic echocardiography (Sonos5500, PHILIPS) was performed day 5, 4 weeks and 16 weeks post-MI. Left ventricular (LV) diastolic dimension (LVDd) and systolic dimension (LVDs) and fractional shortening (FS) were measured at the mid-papillary muscle level [30, 31]. All measurements were examined by an expert researcher (J. D.) who was blinded to treatment.

2.6 Angiogenesis assay

Sixteen weeks post-MI, the samples were fixed with 4% PFA and were stained for rat-specific endothelial cell marker isolectin B4 (Vector Laboratories) using alkaline phosphatase for visualizing avidin. Capillary density was evaluated morphometrically by histological examination of five randomly selected fields (×200) of tissue sections of peri-infarct LV myocardium. Capillaries were recognized as tubular structures positive for isolectin B4[18].

2.7 Dual-radiotracer microSPECT-CT imaging

A subset of animals was sent to Yale University School of Medicine for molecular targeted microSPECT-CT imaging of angiogenesis at 4 and 16 weeks post MI. Rats were anesthetized with 1–3% isofluorane, and the left jugular vein was isolated for placement of a polyethylene catheter (PE-50, Beckton-Dickinson) to facilitate injection of radiotracers. All animals (AAV-IGF-1, n=10: and AAV-lacZ, n=9) were injected intravenously with 6.42±0.46mCi of ^{99m}Tc-labeled chelate-peptide conjugate containing an RGD (Arg-Gly-Asp) motif (^{99m}Tc-NC100692) targeted at αv integrin at 4 weeks (n=8) and 16 weeks (n=11) post-MI. Imaging was performed using hybrid small animal microSPECT-CT scanner (X-SPECT, GammaMedica-Ideas, Northridge, CA) equipped with 1-mm pinhole collimators. Animals were placed on the animal bed, and 75 minutes after radiotracer injection microSPECT imaging (32 projections, 60 sec/projection per head) with a 20% energy window centered at 140 keV was performed. This was followed by intravenous injection of ^{201}Tl chloride (0.81±0.06mCi) and repeated microSPECT imaging with a 15% energy window centered at 78 keV was performed. This was followed by a high-resolution anatomical microCT imaging (512 projections, 50kVp/600μA energy) during continuous infusion of an iodinated X-ray contrast (Omnipaque, GE Healthcare) at a constant rate (0.6 mL/min) using a computer-controlled syringe pump. After the last imaging session, animals were euthanized with intravenous injection of potassium chloride.

2.8 Gamma-well counting

Rats were euthanized immediately after in vivo microSPECT-CT imaging, the hearts were quickly excised, and cleaned with ice-cold saline solution. The excised hearts were filled with dental molding material (alginate impression material, Quala Dental Products) to facilitate uniform cutting into 2-mm thick slices. The slices were photographed and cut into 8 transmural segments and weighed for GWC.

Tissue ^{201}Tl, and ^{99m}Tc activity was measured with gamma-well counter (Cobra Packard) using appropriate energy windows (half-max width of corresponding photopeaks of 78keV and 140keV for ^{201}Tl and ^{99m}Tc, respectively). Raw counts were corrected for spill-up/spill-

down, background, decay, and weight. Corrected counts were converted to mCi/g by use of a previously determined counter efficiency. Based on gross pathological appearance and location myocardial segments were segregated into one of three categories: infarct, border, or remote. Activity in each myocardial segment was calculated as percentage of injected dose per weight (%ID/g). For this calculation, the tissue activity was corrected for decay to the time of radiotracer injection.

2.9 Statistical Analysis

The means and standard errors (SE) were determined for replicate samples. For GWC analysis, the mean and SE of samples have been calculated and expressed in %ID/g. Unpaired Student's t-test was performed to calculate the statistical significance between the means of two groups and between infarct, border and remote in GWC analysis.

3. Results

3.1 AAV-mediated IGF-1 expression in cardiac cells and tissues

We initially overexpressed the AAV-IGF-1 vector containing human IGF-1 gene in cultured rat H9C2 cells. H9C2 cells were infected with 1000 particles per cell of AAV-IGF-1, and mRNA expression of human IGF-1 was examined by RT-PCR. IGF-1 was strongly expressed in a time dependent manner through the AAV vector system (Fig.1A). To evaluate whether the exogenous IGF-1 expression affects the infected cells, we analyzed Akt, an important effector on angiogenesis [32], after infection of control AAV-lacZ vector, AAV-IGF-1 vector or AAV-GH vector [18]. Both AAV-IGF-1 and AAV-GH upregulated gene expression of Akt1 by 5.7-fold and 2.4-fold in H9C2 cells, respectively (Fig.1B). These results suggest that AAV can mediate IGF-1 expression.

To examine the in vivo induction of IGF-1 expression by AAV in an infarcted heart, we employed an established rat model of MI[18]. A total of 1×10^{11} AAV-lacZ or AAV-IGF-1 vectors were delivered by direct injection to five different portions of the peri-infarct area as previously described [18]. The concentration of human IGF-1 in serum of rats was measured by hIGF-1-ELISA. Although there were no elevations of hIGF-1 in the AAV-lacZ control group, circulating hIGF-1 levels were significantly increased at both 4 weeks and 16 weeks after injection of AAV-IGF-1 (Fig.1C). These results suggest that the AAV-IGF-1 vector significantly transduced expression of IGF-1 in the heart.

To verify gene transfer following AAV injection, total DNA was isolated from the heart, and the presence of AAV genomes was analyzed by regular PCR. Agarose gel electrophoresis demonstrated the 286-bp band related to AAV genome sequence, which shows an inverted terminal repeat (ITR) in AAV-lacZ- or in AAV-IGF-1-infected tissues, although PBS-injected heart did not demonstrate this band (Fig.1D).

3.2 Overexpression of IGF-1 improves cardiac function and reduces post-MI LV remodeling

We tested the physiological effects of AAV-mediated expression of IGF-1 on cardiac dysfunction post-MI. Transthoracic echocardiography demonstrated that at baseline (5 days after infarction), left ventricular diastolic dimension (LVDd), left ventricular systolic dimension (LVDs) and fractional shortening (FS) were similar between the AAV-lacZ control group and the AAV-IGF-1 group (Fig.2). Four weeks post-MI, there were significant differences in LVDd and LVDs between the two groups. Both groups demonstrated significant LV remodeling by 16 weeks post-MI, with significant increases in LVDd and LVDs. However, LVDd and LVDs were significantly ($P<0.01$) lower in the AAV-IGF-1 group (1.09±0.04 and 0.87±0.04cm) compared to the AAV-lacZ group (1.33±0.05 and 1.15±0.04cm), suggesting less LV remodeling. Average FS at 16 weeks post-MI in the AAV-IGF-1 group (20.4±1.6%)

was significantly higher compared to the control group (13.4±1.3%) (Fig.2). These findings indicate that induction of IGF-1 expression by AAV-IGF-1 preserves cardiac function post-MI.

3.3 Angiogenesis induced by overexpression of IGF-1

We examined the relative induction of angiogenesis quantitatively between lacZ group and IGF-1 group at 4 weeks and 16 weeks post-MI. Immunohistochemical analysis revealed that capillary density of the heart in AAV-IGF-1 group (4 weeks: 162.9±10.1; 16 weeks: 209.9 ±11.6) was significantly higher than lacZ control group (4 weeks: 96.9±6.04, $p < 0.01$; 16 weeks: 121.5±6.9, $P<0.01$) post-MI (Fig.3A through 3C).

To confirm expression of mRNA for a number of angiogenesis-associated factors, we performed quantitative RT-PCR at 4 and 16 weeks post-MI. Human IGF-1 gene expression was stably upregulated both at 4 and 16 weeks (Fig.4). eNOS mRNA expression was augmented in the IGF-1 group 4 weeks post-MI, although this initial activation was markedly reduced at 16 weeks post-MI (Fig.4). Although overexpression of IGF-1 was associated with an increased gene expression of Akt, VEGF and bFGF at 4 weeks post-MI, the mRNA expression of these critical angiogenic factors was reduced in the IGF-1 treated group relative to the control group at 16 weeks post-MI (Fig.4).

3.4 Dual-radiotracer microSPECT-CT imaging

Dual-isotope microSPECT imaging was performed after injection of ^{99m}Tc-NC100692, and ^{201}Tl, and was followed by microCT imaging after the administration of an intravascular X-ray contrast agent (Omnipaque) to better define both the right and left ventricular myocardium. Representative short and long axes images are shown in a rat subjected to AAV-IGF-1 therapy at 4 weeks post-MI (Fig.5A). Administration of CT contrast improved definition of myocardial edges and demonstrated wall thinning and expansion of the infarct territory along with LV enlargement. ^{201}Tl behaves physiologically as a potassium analog, and when injected intravenously accumulates rapidly within the cells of many organs including heart. The initial uptake of ^{201}Tl within the heart reflects regional myocardial perfusion while retention of the radiotracer reflects integrity of sodium-potassium ATPase pump activity, and therefore also proved an index of myocardial viability. Reduction of regional myocardial uptake of ^{201}Tl results in a cold spot on the myocardial image. ^{201}Tl microSPECT images reproducibly demonstrated an anterolateral perfusion defect, while ^{99m}Tc-NC100692 microSPECT imaging demonstrated a focal uptake of the targeted radiotracer within the infarct (defined by perfusion defect), as well as in the chest wall at the site of the thoracotomy. This relationship between the two radiotracers was best seen in the fused contrast microCT (grayscale) and microSPECT images (red: ^{99m}Tc-NC100692; and green: ^{201}Tl). The use of microCT contrast images greatly enhanced our ability to reconstruct and reorient the registered microSPECT images without the reference ^{201}Tl images, which in several animals were of suboptimal quality. The microSPECT-CT images consistently demonstrated uptake of ^{99m}Tc-NC100692 within the site of the ^{201}Tl perfusion defect, confirming localization of principal αv integrin activation to the MI region.

3.5 Gamma-Well Counting

The significant increase in ^{99m}Tc-NC100692 retention within the infarct territory that was observed with microSPECT-CT imaging was confirmed by GWC of myocardial tissue sections. GWC permitted quantification of absolute myocardial ^{99m}Tc-NC100692 retention expressed as %ID/g in relationship to myocardial perfusion. Increased myocardial retention of ^{99m}Tc-NC100692 was seen in anteriolateral wall in the area of decreased ^{201}Tl retention. Representative myocardial radiotracer count profiles are shown in Fig.5B.

The GWC results from AAV-IGF-1-treated and control AAV-lacZ rats at 4 and 16 weeks post-MI are summarized in Fig.6. All myocardial segments were segregated into infarct, border, and remote regions. In all post-MI animals there was a significant increase of ^{99m}Tc-NC100692 retention in infarct territory compared to remote non-ischemic regions. At 4 weeks post-MI, AAV-IGF-1 treated rats demonstrated significant increase in ^{99m}Tc-NC100692 uptake in all myocardial regions as compared to AAV-lacZ rats (Fig.6A) suggesting global activation of αv integrins. At 16 weeks post-MI, the myocardial ^{99m}Tc-NC100692 retention within infarct regions was ~31% lower in AAV-IGF-1 rats compared to AAV-lacZ control rats (Fig.6B). A similar trend was observed in the other non-infarcted myocardial regions.

4. Discussion

In this study, we demonstrated that local delivery of IGF-1 gene by recombinant AAV in the setting of acute MI resulted in sustained IGF-1 expression, increased angiogenesis, reduced LV-remodeling and improved cardiac function. The effect of AAV-IGF-1 treatment on angiogenesis was examined using an established rat model of MI with both in vitro biochemical assays for a number of angiogenic factors, and in vivo microSPECT-CT imaging using a ^{99m}Tc-labeled peptide targeted at αv integrins, known to be activated during the angiogenic process [23].

We recently reported that growth hormone (GH) expression by AAV significantly improved cardiac function and induced angiogenesis post-MI using the same rat model [18]. Both AAV-IGF-1 and AAV-GH vectors significantly induced gene expression of Akt in the rat, however, the IGF-1 vector has been shown to induce Akt more than the GH vector (Fig.1B). Other investigators demonstrated that IGF-1 is also a potent effector of GH [33]. Chao et al. reported that overexpression of human IGF-1 gene by adenovirus in the rat model of MI resulted in a reduction of the infarct size 24-hours post-MI [34]. Adenovirus-mediated gene transfer can result in high levels of transduction, however, the transduction can only be preserved temporarily due to absence of integration to chromosome in the host cells and induction of severe immunoreaction. Accordingly, we used AAV-IGF-1 vector for the present study and observed stable expression of IGF-1 up to 16 weeks post-infection without detection of inflammation in the samples (Fig.1C). Regarding the therapeutic value of the AAV-IGF-1 vector post-MI, we did demonstrate an improvement of cardiac function and reduced LV remodeling with sustained induction of IGF-1 (Fig.2), therefore our findings strongly support the results of the previous experiments [34].

In the current study, we demonstrated an increase in capillary number in the hearts following AAV-IGF-1 treatment that was greater than the AAV-lacZ treated rats at 4 and 16 weeks post-MI, indicating that IGF-1 expression can significantly enhance angiogenesis in infarcted hearts (Fig.3A through 3C). However, there was no significant change in the capillary number between 10 and 16 weeks in the AAV-lacZ treated rats (data not shown). This suggests that AAV-mediated IGF-1 expression induces angiogenesis in the early stage after injection and may not augment the capillary number during the later phases of post-MI remodeling.

Akt, eNOS, VEGF and bFGF gene expression have been reported as important proangiogenic factors [26,27,32,35]. In our study the mRNA expression of these angiogenic factors was much greater after AAV-IGF-1 vector infection compared to control (Fig.4), indicating that these factors may play an important role in IGF-1-induced capillary formation. At 16 weeks after infection, the gene expression of Akt, VEGF and bFGF was prominently downregulated under the condition of sustained IGF-1 overexpression, relative to the control group. Previously, we reported GH-induced angiogenesis through upregulation of VEGF and bFGF [18]. This earlier study also demonstrated increased VEGF and bFGF gene expression over control rats at 4 weeks post-MI but not at a later time point [18]. Taken together, these results suggest that both

GH and IGF-1 expression have a limited capacity to enhance angiogenesis in the later stages post-MI. It is also plausible that the increase in capillary density is driven by the degree of ischemia, and plateaus when sufficient perfusion is restored.

We employed targeted molecular imaging using a radiolabeled tracer targeted at the αv integrins. This targeted imaging approach has recently emerged as a new non-invasive method for assessment of the angiogenic process in vivo [20,22,36,37]. In particular, the αv integrins belong to the transient cell surface markers which may be used to differentiate angiogenic vessels from mature capillaries. In previously published studies we have demonstrated that ^{99m}Tc-labeled NC100692 containing the RGD motif preferentially binds to activated αv integrins including the αvβ3 integrin (vitronectin receptor), a well-recognized biomarker of angiogenesis [20,37]. In this study we used ^{99m}Tc-NC100692 to assess temporal and spatial changes in myocardial angiogenesis between control (AAV-lacZ) and AAV-IGF-1 treated rats post-MI. In the current study, ^{99m}Tc-NC100692 was selectively retained in the infarcted myocardial regions with reduced ^{201}Tl perfusion (Fig.5) suggesting ongoing ischemia-stimulated angiogenesis. Using hybrid microSPECT-CT imaging we were able to define focal myocardial retention of the αv integrin targeted radiotracer from retention within chest wall at the thoracotomy site (Fig.5A) reflective of the angiogenesis associated with wound healing. The image-based analysis was validated with quantitative analysis of ^{99m}Tc-NC100692 activity within myocardium using gamma-well counting of myocardial sections. The myocardial sections were segregated into infarct, border, and remote regions based on gross pathological appearance and location (Fig.5B).

In our previous imaging studies in evaluation of naturally occuring ischemia-induced myocardial angiogenesis, we have demonstrated that significant retention of a radiolabeled marker of angiogenesis targeted at the αv integrin within the infarct was observed as early as a few hours post LAD ligation [21] and was detected as late as 2 weeks post-MI [22]. These earlier studies employed a radiolabeled peptidomimetic targeted at the αv integrin, while the current study employs a radiolabeled cyclic RGD peptide. In the current study involving therapeutic angiogenesis, there was over a two-fold increase in relative myocardial ^{99m}Tc-NC100692 retention in infarcted tissue in both AAV-IGF-1 treated and control rats at 4 and 16 weeks post-MI compared with remote non-infarcted regions (Fig.6A). At 4 weeks post-MI, we observed a significant increase in ^{99m}Tc-NC100692 in AAV-IGF-1 rats in infarct, border, and remote sections compared to AAV-lacZ control rats (Fig.6A). These changes were similar to those observed in mRNA expression of other biochemical markers (Akt, eNOS, VEGF, and bFGF) reflective of the angiogenic process. Interestingly, there was a significant increase in ^{99m}Tc-NC100692 retention in all myocardial regions, suggesting a global effect of AAV-IGF-1 treatment on early αv integrin activation within the myocardium. In contrast, AAV-IGF-1 rats at 16 weeks post-MI demonstrated a significant reduction in ^{99m}Tc-NC100692 retention in all regions compared to AAV-lacZ rats. The AAV-IGF-1 treated rats demonstrated a greater than 30% decrease in absolute ^{99m}Tc-NC100692 retention within the infarct region, which was paralleled by decreases in other non-infarcted myocardial segments (Fig.6B). This reduction of αv integrin activation at 16 weeks post-MI matched the observed decrease in mRNA expression of Akt, VEGF, and bFGF. This suggests primarily an acute effect of AAV-IGF-1 on stimulation of the angiogenic process post-MI. Although the IGF-1 serum concentration, capillary density, and eNOS mRNA expression were elevated at the later time point, the angiogenic process appears to have been “shut-off” in AAV-IGF-1 group at 16 weeks post-MI. The absolute ^{99m}Tc-NC100692 retention within the infarct of the AAV-IGF-1 group at 16 weeks returned to the level observed in remote regions at 4 weeks post-MI.

In conclusion, we have demonstrated that intramyocardial delivery of AAV-IGF-1 in the peri-infarct area during acute MI resulted in sustained IGF-1 expression, and promoted successful myocardial angiogenesis in the early phase of post-MI repair as evidenced by

immunohistochemistry, biochemical markers of angiogenesis and molecular microSPECT-CT imaging using radiolabeled tracer targeted at αv integrins. AAV-IGF-1 treatment was also successful in inhibiting late post-MI myocardial remodeling and maintaining cardiac function as assessed by serial echocardiography.

This study demonstrates that the targeted imaging of ischemia-induced angiogenesis provides a novel approach for the assessment of therapeutic angiogenesis in combination with measurements of biochemical markers of neovascularization. The proposed combined imaging-biomarker approach may provide a new strategy in clinical trials to evaluate genetic or stem cell therapies directed at stimulating angiogenesis in patients with ischemic heart disease.

Acknowledgments

We thank Dr Douglas Losordo for support. This work was supported by Starr foundation grant (RA) and NIH grant R01 HL65662 (AS).

References

1. Liu JL, Yakar S, LeRoith D. Mice deficient in liver production of insulin-like growth factor I display sexual dimorphism in growth hormone-stimulated postnatal growth. Endocrinology 2000;141(22): 4436–4441. [PubMed: 11108252]
2. Khan AS, Sane DC, Wannenburg T, Sonntag WE. Growth hormone, insulin-like growth factor-1 and the aging cardiovascular system. Cardiovasc Res 2002;54(1):25–35. [PubMed: 12062358]
3. Delafontaine P, Song YH, Li Y. Expression, regulation, and function of IGF-1, IGF-1R, and IGF-1 binding proteins in blood vessels. Arterioscler Thromb Vasc Biol 2004;24(3):435–444. [PubMed: 14604834]
4. Li Q, Li B, Wang X, Leri A, Jana KP, Liu Y, et al. Overexpression of insulin-like growth factor-1 in mice protects from myocyte death after infarction, attenuating ventricular dilation, wall stress, and cardiac hypertrophy. J Clin Invest 1997;100(8):1991–1999. [PubMed: 9329962]
5. Welch S, Plank D, Witt S, Glascock B, Schaefer E, Chimenti S, et al. Cardiac-specific IGF-1 expression attenuates dilated cardiomyopathy in tropomodulin-overexpressing transgenic mice. Circ Res 2002;90 (6):641–648. [PubMed: 11934830]
6. Torella D, Rota M, Nurzynska D, Musso E, Monsen A, Shiraishi I, et al. Cardiac stem cell and myocyte aging, heart failure, and insulin-like growth factor-1 overexpression. Circ Res 2004;94(4):514–524. [PubMed: 14726476]
7. Schulze PC, Fang J, Kassik KA, Gannon J, Cupesi M, MacGillivray C, et al. Transgenic overexpression of locally acting insulin-like growth factor-1 inhibits ubiquitin-mediated muscle atrophy in chronic left-ventricular dysfunction. Circ Res 2005;97(5):418–426. [PubMed: 16051886]
8. Su EJ, Cioffi CL, Stefansson S, Mittereder N, Garay M, Hreniuk D, et al. Gene therapy vector-mediated expression of insulin-like growth factors protects cardiomyocytes from apoptosis and enhances neovascularization. Am J Physiol Heart Circ Physiol 2003;284(4):H1429–H1440. [PubMed: 12505877]
9. Lopez-Lopez C, LeRoith D, Torres-Aleman I. Insulin-like growth factor I is required for vessel remodeling in the adult brain. Proc Natl Acad Sci U S A 2004 Jun 29;101(26):9833–9838. 2004; 101 (26). [PubMed: 15210967]
10. Rabinovsky ED, Draghia-Akli R. Insulin-like growth factor I plasmid therapy promotes in vivo angiogenesis. Mol Ther 2004;9(1):46–45. [PubMed: 14741777]
11. Jabri N, Schalch DS, Schwartz SL, Fischer JS, Kipnes MS, Radnik BJ, et al. Adverse effects of recombinant human insulin-like growth factor I in obese insulin-resistant type II diabetic patient. Diabetes 1994;43(3):369–374. [PubMed: 8314009]
12. Su H, Lu R, Kan YW. Adeno-associated viral vector-mediated vascular endothelial growth factor gene transfer induces neovascular formation in ischemic heart. Proc Natl Acad Sci U S A 2000;97 (25):13801–13806. [PubMed: 11095751]

13. Melo LG, Agrawal R, Zhang L, Rezvani M, Mangi AA, Ehsan A, et al. Gene therapy strategy for long-term myocardial protection using adeno-associated virus-mediated delivery of heme oxygenase gene. Circulation 2002;105(5):602–607. [PubMed: 11827926]

14. Hoshijima M, Ikeda Y, Iwanaga Y, Minamisawa S, Date MO, Gu Y, et al. Chronic suppression of heart-failure progression by a pseudophosphorylated mutant of phospholamban via in vivo cardiac rAAV gene delivery. Nat Med 2002;8(8):864–871. [PubMed: 12134142]

15. Snyder RO, Spratt SK, Lagarde C, Bohl D, Kaspar B, Sloan B, et al. Efficient and stable adeno-associated virus-mediated transduction in the skeletal muscle of adult immunocompetent mice. Hum Gene Ther 1997;8(16):1891–1900. [PubMed: 9382955]

16. Fisher KJ, Jooss K, Alston J, Yang Y, Haecker SE, High K, et al. Recombinant adeno-associated virus for muscle directed gene therapy. Nat Med 1997;3(3):306–312. [PubMed: 9055858]

17. Aikawa R, Huggins GS, Snyder RO. Cardiomyocyte-specific gene expression following recombinant adeno-associated viral vector transduction. J Biol Chem 2002;277(21):18979–18985. [PubMed: 11889137]

18. Kusano K, Tsutsumi Y, Dean J, Gavin M, Ma H, Silver M, et al. Long-term stable expression of human growth hormone by rAAV promotes myocardial protection post-myocardial infarction. J Mol Cell Cardiol 2007;42:390–399. [PubMed: 17174322]

19. Hua J, Dobrucki LW, Sadeghi MM, Zhang J, Bourke BN, Cavaliere P, et al. Noninvasive imaging of angiogenesis with a 99mTc-labeled peptide targeted at alphavbeta3 integrin after murine hindlimb ischemia. Circulation 2005 Jun 21;111(24):3255–3260. [PubMed: 15956134]

20. Lindsey ML, Escobar GP, Dobrucki LW, Goshorn DK, Bouges S, Mingoia JT, et al. Matrix metalloproteinase-9 gene deletion facilitates angiogenesis after myocardial infarction. Am J Physiol Heart Circ Physiol 2006 Jan;290(1):H232–H239. [PubMed: 16126817]

21. Kalinowski L, Dobrucki LW, Meoli DF, Dione DP, Sadeghi MM, Madri JA, et al. Targeted imaging of hypoxia-induced integrin activation in myocardium early after infarction. J Appl Physiol 2008 May;104(5):1504–1512. [PubMed: 18356482]

22. Meoli DF, Sadeghi MM, Krassilnikova S, Bourke BN, Giordano FJ, Dione DP, et al. Noninvasive imaging of myocardial angiogenesis following experimental myocardial infarction. J Clin Invest 2004 Jun;113(12):1684–1691. [PubMed: 15199403]

23. Edwards D, Jones P, Haramis H, Battle M, Lear R, Barnett DJ, et al. 99mTc-NC100692--a tracer for imaging vitronectin receptors associated with angiogenesis: a preclinical investigation. Nucl Med Biol 2008 Apr;35(3):365–375. [PubMed: 18355693]

24. Iwakura A, Dean J, Hamada H, Eaton E, Qin G, Losordo DW, et al. Use of recombinant adenoassociated viral vectors as a tool for labeling bone marrow cells. J Mol Cell Cardiol 2005;38:799–802. [PubMed: 15850573]

25. Losordo DW, Dimmeler S. Therapeutic angiogenesis and vasculogenesis for ischemic disease. Part I: angiogenic cytokines. Circulation 2004;109(21):2487–2491. [PubMed: 15173038]

26. Losordo DW, Vale PR, Symes JF, Dunnington CH, Esakof DD, Maysky M, et al. Gene therapy for myocardial angiogenesis: initial clinical results with direct myocardial injection of phVEGF165 as sole therapy for myocardial ischemia. Circulation 1998;98(25):2800–2804. [PubMed: 9860779]

27. Horvath KA, Doukas J, Lu CY, Belkind N, Greene R, Pierce GF, et al. Myocardial functional recovery after fibroblast growth factor 2 gene therapy as assessed by echocardiography and magnetic resonance imaging. Ann Thorac Surg 2002;74(2):481–486. [PubMed: 12173832]

28. Spyridopoulos I, Luedemann C, Chen D, Kearney M, Murohara T, Principe N, et al. Divergence of angiogenic and vascular permeability signaling by VEGF: inhibition of protein kinase C suppresses VEGF-induced angiogenesis, but promotes VEGF-induced, NO-dependent vascular permeability. Arterioscler Thromb Vasc Biol 2002;22(6):901–906. [PubMed: 12067896]

29. Dimmeler S, Zeiher AM. Akt Takes Center Stage in Angiogenesis Signaling. Circ Res 2000 January 7;86(1):4–5. 2000. [PubMed: 10625297]

30. Kawamoto A, Gwon HC, Iwaguro H, Yamaguchi JI, Uchida S, Masuda H, et al. Therapeutic potential of ex vivo expanded endothelial progenitor cells for myocardial ischemia. Circulation 2001;103(5): 634–637. [PubMed: 11156872]

31. Yoon YS, Wecker A, Heyd L, Park JS, Tkebuchava T, Kusano K, et al. Clonally expanded novel multipotent stem cells from human bone marrow regenerate myocardium after myocardial infarction. J Clin Invest 2005;115(2):326–338. [PubMed: 15690083]

32. Takahashi A, Kureishi Y, Yang J, Luo Z, Guo K, Mukhopadhyay D, et al. Myogenic Akt signaling regulates blood vessel recruitment during myofiber growth. Mol Cell Biol 2002;22(13):4803–4814. [PubMed: 12052887]

33. Khan AS, Lynch CD, Sane DC, Willingham MC, Sonntag WE. Growth hormone increases regional coronary blood flow and capillary density in aged rats. J Gerontol A Biol Sci Med Sci 2001;56 (8):B364–B371. [PubMed: 11487595]

34. Chao W, Matsui T, Novikov MS, Tao J, Li L, Liu H, et al. Strategic advantages of insulin-like growth factor-I expression for cardioprotection. J Gene Med 2003;5(4):277–286. [PubMed: 12692862]

35. Michell BJ, Griffiths JE, Mitchelhill KI, Rodriguez-Crespo I, Tiganis T, Bozinovski S, et al. The Akt kinase signals directly to endothelial nitric oxide synthase. Curr Biol 1999;9(15):845–848. [PubMed: 10469573]

36. Dobrucki L, Hua J, Bourke B, Sadeghi M, Cavaliere P, Mendizabal M, et al. Non-invasive imaging of hypoxia induced angiogenesis following hindlimb ischemia in mice. J Nucl Cardiol 2004;11:372.

37. Hua J, Dobrucki L, Sadeghi M, Zhang J, Bourke B, Cavaliere P, et al. Noninvasive imaging of angiogenesis with a 99mTc-labeled peptide targeted at αvβ3 integrin after murine hindlimb ischemia. Circulation 2005;111:3255–3260. [PubMed: 15956134]

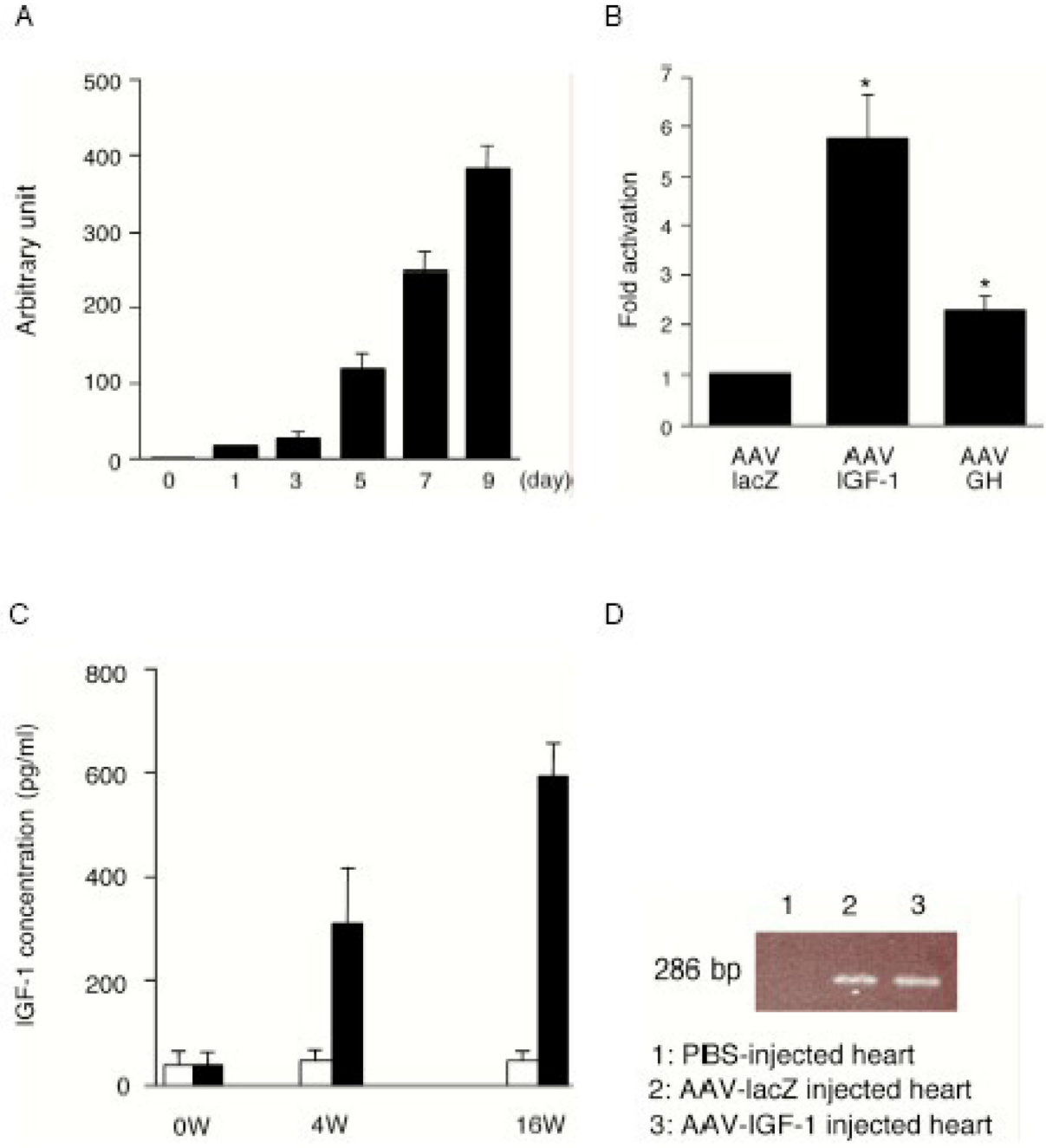

Fig. 1.

(A) IGF-1 gene expression induced with AAV in cultured cells. After infection of AAV-CMV-IGF-1 into rat H9C2 cells under the indicated time course, total RNA from cells was extracted and analysed by quantitative real time (RT)-PCR using human IGF-1 primers.

(B) Rat Akt1 gene expression. AAV-CMV-lacZ, AAV-CMV-IGF-1 or AAV-CMV-GH was infected into H9C2 cells, and 7 days after infection, each mRNA was examined by RT-PCR using rat Akt1 primers. (n=4) *P<0.05 vs. AAV-lacZ.

(C) Long term expression of AAV-CMV-IGF-1. After ligation of coronary artery, total 1×10^{11} AAV vectors were injected into myocardium. The serum concentration of human IGF-1

in AAV-infected rats was measured by ELISA. White columns show the AAV-lacZ group and black columns show the AAV-IGF-1 group.
(D) PCR amplification of rAAV genome from infected hearts 16 weeks after infection. The primers were designed for a 286-bp fragment from ITR region to CMV promoter. Lane 1, non-rAAV-infected heart; Lane 2, AAV-lacZ infected heart; Lane 3, AAV-IGF-1 infected heart.

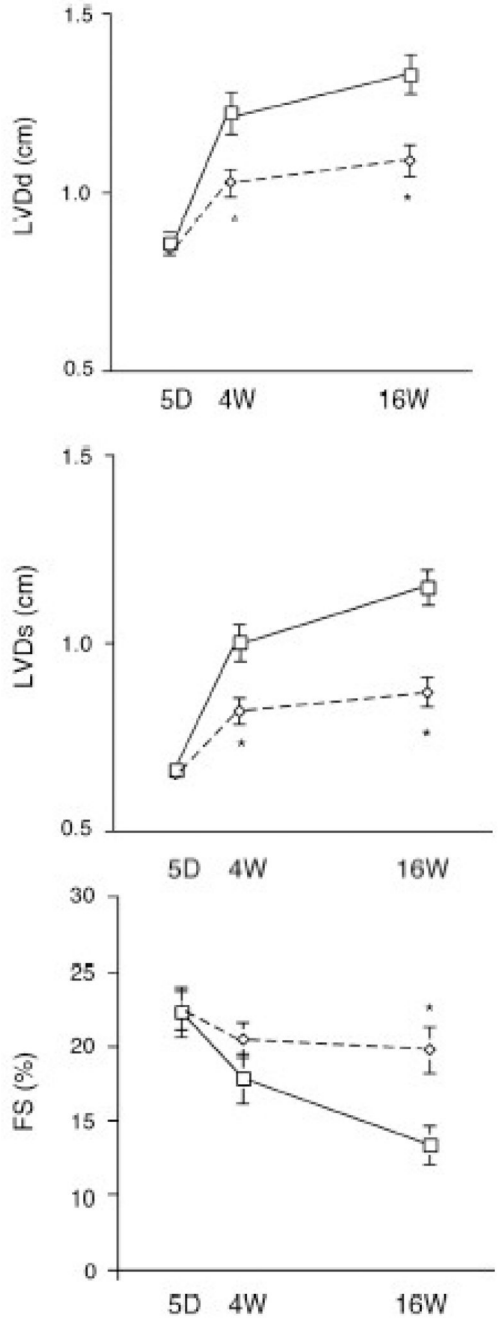

Fig. 2.

Serial changes in transthoracic echocardiographic parameters from baseline (day 5) to 4 and 16 weeks post-MI and vector therapy. Dotted lines indicate rats treated with rAAV-IGF-1 vectors: solid lines; control lacZ group. (n=8 in both groups) *P<0.01, vs. control lacZ group.

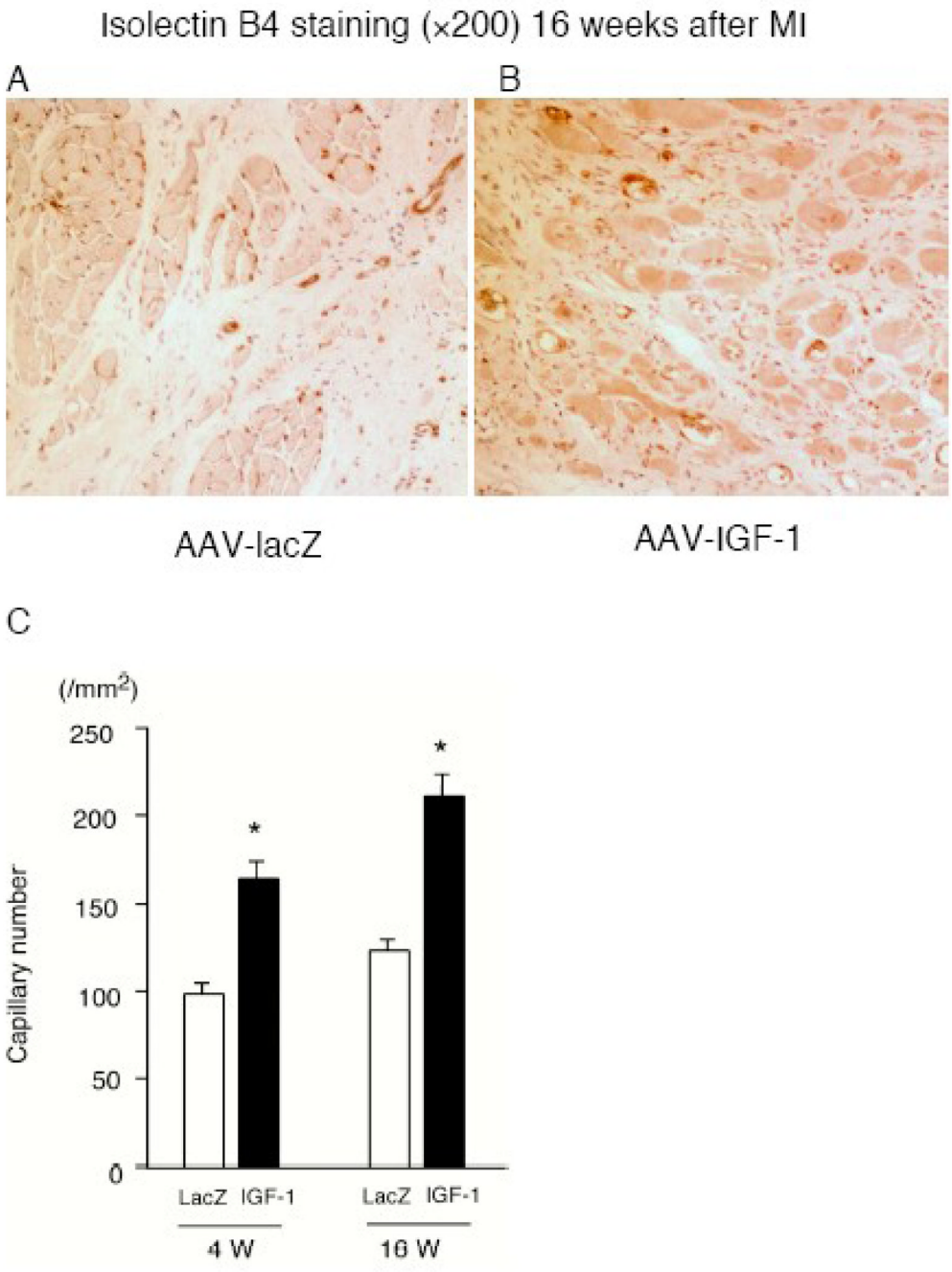

Fig. 3.

(A) and (B) immunohistochemistry using an anti-isolectin B4 at 16 weeks post-MI. (C) Capillary density in rats receiving AAV-lacZ or AAV-IGF. (n=8) *P<0.01 vs. control lacZ.

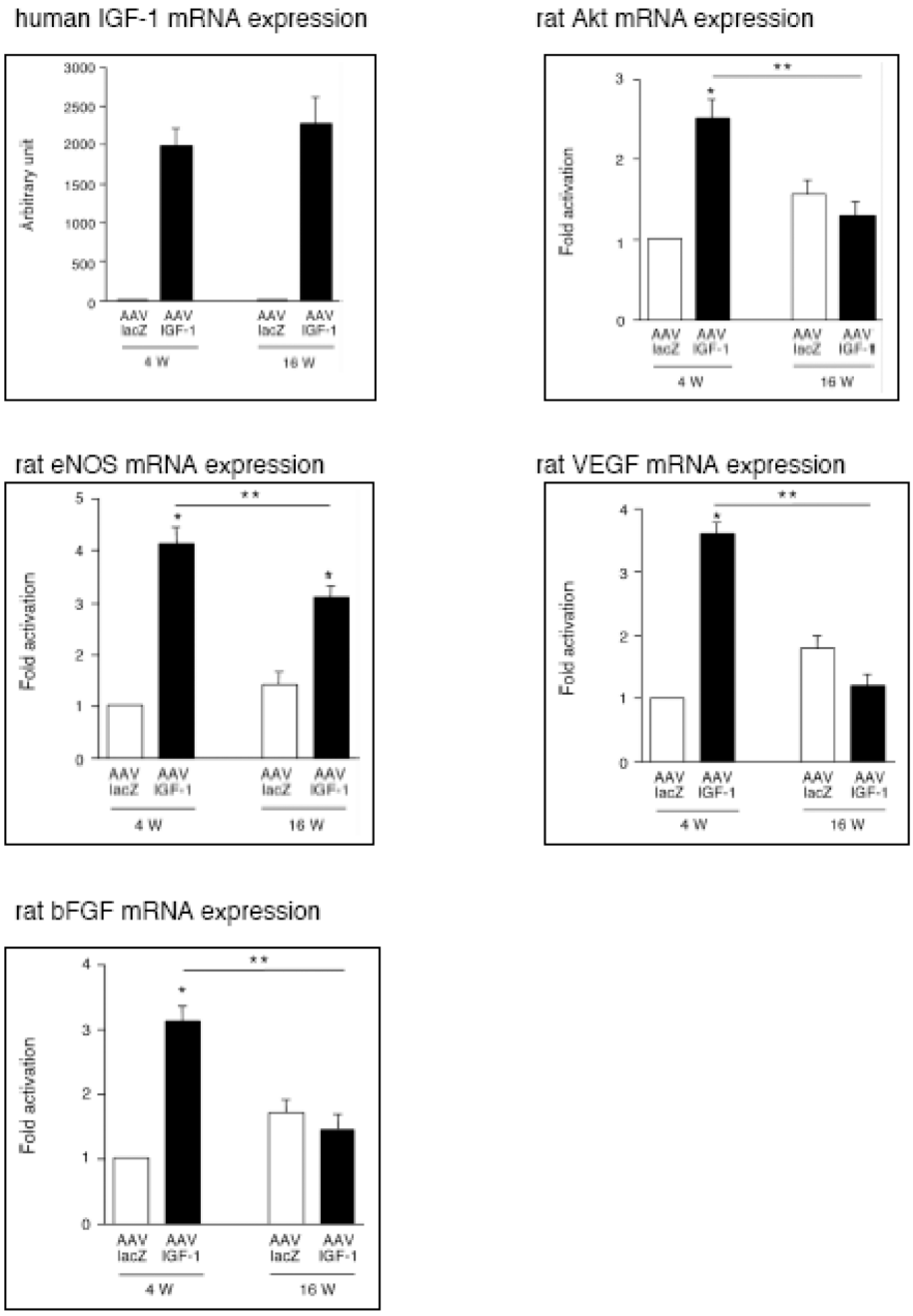

Fig. 4.

IGF-1 promotes mRNA expression of angiogenic factors in AAV-infected hearts. mRNA level of human IGF-1, rat Akt1, rat eNOS, rat VEGF-A, and rat bFGF was assessed by quantitative RT- PCR and expressed as ratio of each factor normalized with GAPDH. (n=6) *P<0.01 vs. lacZ group, **P<0.05 vs. 4 weeks

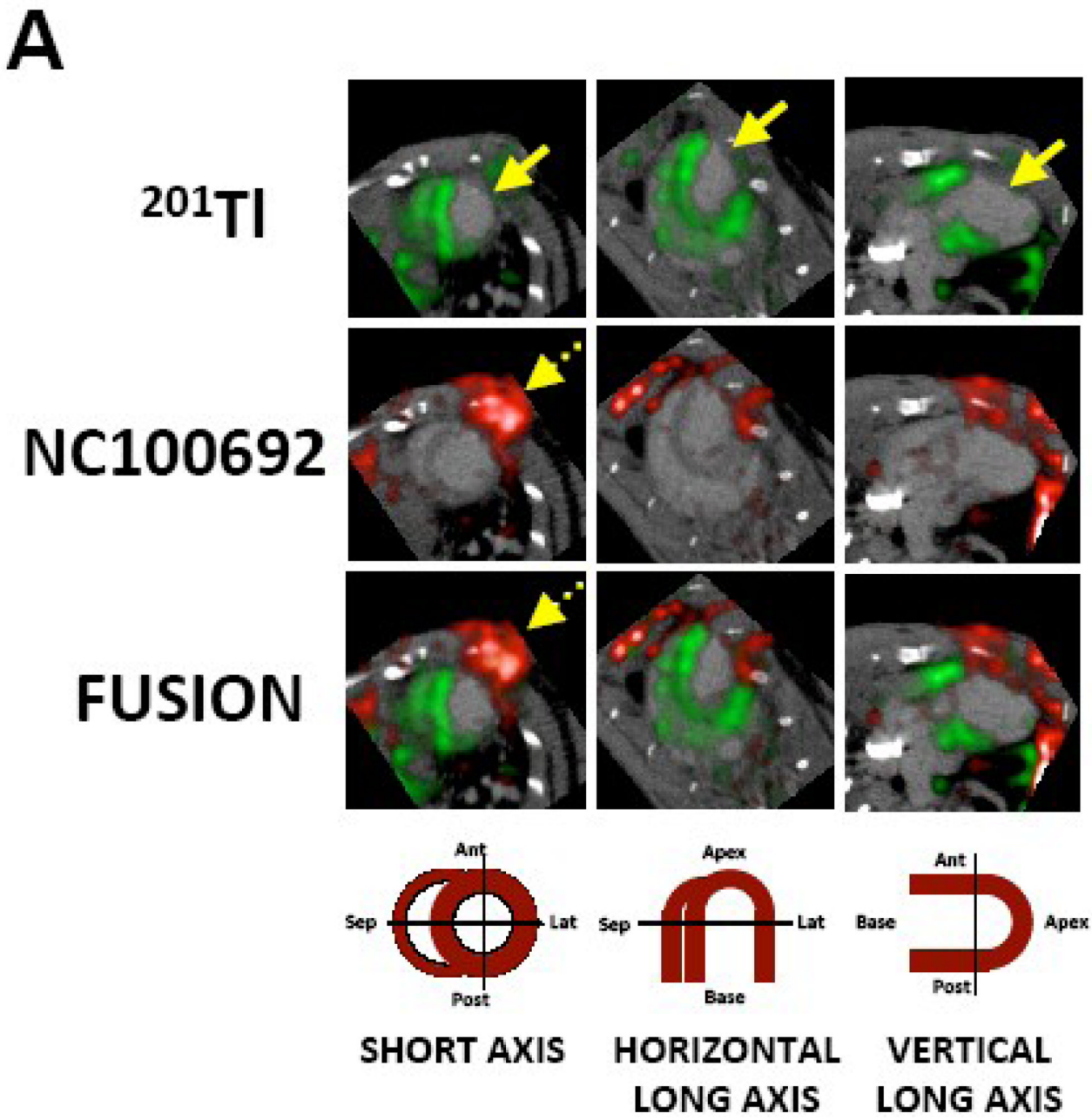

Fig. 5.

(A) In vivo microSPECT-CT images of ^{201}Tl perfusion (top row, green) and ^{99m}Tc-NC100692 (middle row, red) in IGF-1 rat at 4 weeks post-MI were reconstructed in short and horizontal and vertical long axes and fused (bottom row) with a reference contrast CT image (grayscale). All post-MI rats had an anterolateral ^{201}Tl perfusion defect (yellow solid arrows) and focal uptake of ^{99m}Tc-NC100692 in defect area. The contrast agent permitted better definition of myocardium allowing differentiation of focal myocardial uptake of targeted radiotracer from uptake within chest wall at the thoracotomy site (dashed yellow arrows).

(B) Representative circumferential count profile of middle myocardial section of IGF-1 rat at 4 weeks post-MI. Count profiles for both ^{99m}Tc-NC100692 (solid circles) and ^{201}Tl perfusion (open circles) are demonstrated.

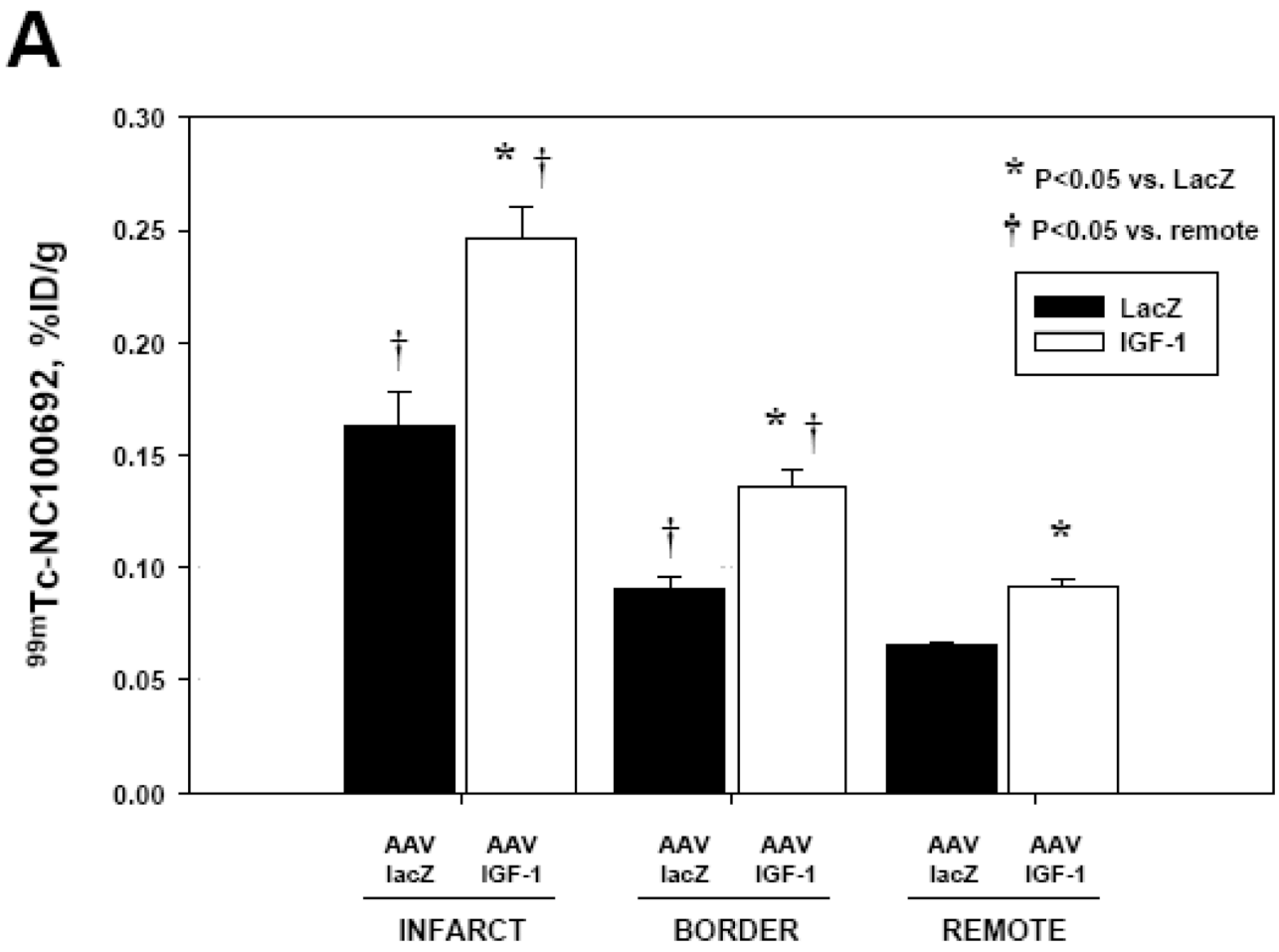

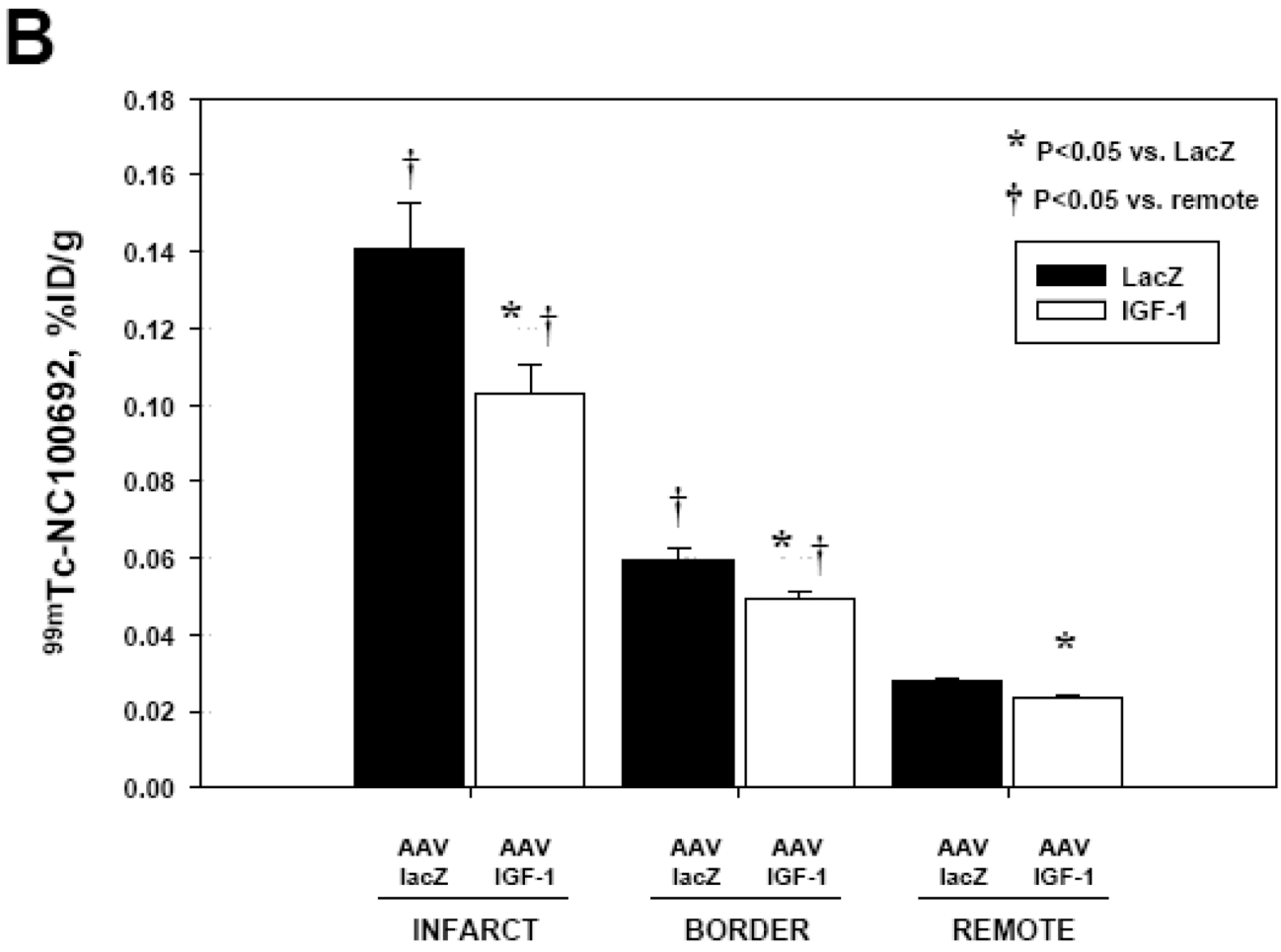

Fig. 6.

Absolute retention of ^{99m}Tc-NC100692 (%ID/g) within myocardium was determined by GWC.

(A) ^{99m}Tc-NC100692 retention in IGF-1 (n=5) and lacZ-control (n=3) rats at 4 weeks post-MI. There was a significant increase in retention of ^{99m}Tc-NC100692 within infarct territory of all animals compared to remote segments. This increase in ^{99m}Tc-NC100692 was significantly higher in IGF-1 animals than in lacZ-controls. This trend was true for all myocardial territories.

(B) ^{99m}Tc-NC100692 retention at 16 weeks post-MI was significantly reduced in IGF-1 animals (n=5) compared to lacZ rats (n=6). The trend for increased ^{99m}Tc-NC100692 retention in IGF-1 treated rats was also observed in border and remote regions.

*P<0.05 vs. lacZ, †P<0.05 vs. remote

Table 1

Oligonucleotide primers used for gene expression analysis by real-time PCR

Gene	Primer Sequences (5'-3')
Human IGF-1	Fwd CCATGTCCTCCTCGCATCTC
	Rev CGTGGCAGAGCTGGTGAAG
	Probe FAM-ACCTGGCGCTGTGCCTGCTCA-BHQ
Rat Akt1	Fwd ACGACCGCCTCTGCTTTG
	Rev ACACGCGCTCACGAGACA
	Probe FAM-CCAATGGAGGCGAGCTCTTCTTCCA-BHQ
GAPDH	Fwd AATGTATCCGTTGTGGATCTGACA
	Rev CCTGCTTCACCACCTTCTTGA
	Probe FAM-CCGCCTGGAGAAACCTGCCAAGTATG-BHQ

VEGF, bFGF and eNOS primers are shown in [Ref. 18].